

Refined structural theories for dynamic analysis of composite structures subjected to random excitation

Original

Refined structural theories for dynamic analysis of composite structures subjected to random excitation / Tortorelli, E.; Filippi, M.; Pagani, A.; Petrolo, M.; Carrera, E.. - (2023). (Intervento presentato al convegno 9th International Conference on Fatigue of Composites, ICFC9 tenutosi a Vicenza nel 21-23 June 2023).

Availability:

This version is available at: 11583/2979610 since: 2023-06-27T07:13:04Z

Publisher:

Marino Quaresimin

Published

DOI:

Terms of use:

This article is made available under terms and conditions as specified in the corresponding bibliographic description in the repository

Publisher copyright

(Article begins on next page)

REFINED STRUCTURAL THEORIES FOR DYNAMIC ANALYSIS OF COMPOSITE STRUCTURES SUBJECTED TO RANDOM EXCITATION

E. Tortorelli^{*}, M. Filippi¹, A. Pagani², M. Petrolo³, E. Carrera⁴

¹Assistant professor, Department of Mechanical and Aerospace Engineering, Politecnico di Torino, Turin, Italy, 10129

²Associate professor, Department of Mechanical and Aerospace Engineering, Politecnico di Torino, Turin, Italy, 10129

³Associate professor, Department of Mechanical and Aerospace Engineering, Politecnico di Torino, Turin, Italy, 10129

⁴Full professor, Department of Mechanical and Aerospace Engineering, Politecnico di Torino, Turin, Italy, 10129

^{*}PhD student, Department of Mechanical and Aerospace Engineering, Politecnico di Torino, Turin, Italy, 10129, elisa.tortorelli@polito.it

Keywords: composite, random excitation, refined structural models.

Abstract

This paper presents the application of the finite element method to analyze the dynamic response of aerospace structures subjected to random excitations. The focus is on using refined structural models to investigate the accuracy of higher-order theories employing the Carrera Unified Formulation (CUF). This formulation enables finite element solutions based on arbitrary kinematic models to be generated with ease. In this paper, the solution scheme is based on the use of power and cross-spectral densities adopting the modal reduction strategy for reducing the computational burden. The response of a sandwich cantilever beam and a laminated beam excited by a white noise are studied. The results prove the ability of refined models to capture dynamic responses at low and high frequencies. Furthermore, higher-order models show a more accurate solution.

1. Introduction

The fatigue phenomenon represents one of the most common causes of failure in structural and mechanical components. It is necessary to introduce the fatigue analysis of real components starting from the estimation of the stress or strain distributions due to the loading history. In this contest, the prediction of the dynamic response of a structure subjected to random excitations is crucial to estimate the fatigue performance. As aircraft and space vehicles encounter gusts and noise excitations during flights [1], a damage tolerance approach can help to compute stresses induced by these loads and to establish if a crack within a component will reach the critical size. Then, fatigue damage is mainly influenced by two factors: fatigue strength of the material and loading history applied. Regarding the loading history applied to a component, a finite time interval is usually experimentally collected and taken as representative due to the impossibility of recording the entire loading history related to a fatigue damage scenario, but different approaches can be applied to characterize the entire domain based on

this extraction. The time- and frequency-domain fatigue approaches can be applied, but the latter procedure is preferred since computationally lighter than the direct integrations of the governing equation in the time domain [2-3]. Therefore, the Power Spectral Density (PSD) approach is a commonly used method in structural dynamics and random vibration analysis [4]. It characterizes the response or loads of a structure in the frequency domain. In this procedure, the structural response and loads are assumed to be stationary and ergodic stochastic processes. The former describes that statistical properties remain constant over time. The latter means that the average statistical properties observed over time for a single realization of the process are representative of the average properties observed across multiple realizations.

The Finite Element Method (FEM) provides a powerful and versatile approach to determine the spectra of displacements and stresses of structures. Many works were based on classical and first-order shear deformation theories [5-8]. While these approaches are suitable for many structural configurations, their underlying assumptions may not be valid for certain applications, such as laminated and thin-walled structures. Employing three-dimensional (3D) solid formulations can overcome these limitations; however, they can often be computationally expensive. In this work, an alternative approach is taken by employing high-order finite beam elements. These elements provide a precise and computationally efficient solution for predicting structural responses resulting from random excitations. The Carrera Unified Formulation (CUF) allows to automatically implement different kinematics by using an opportune recursive notation. The capabilities of one-dimensional CUF elements have been extensively explored in different scenarios, including stress analysis, dynamic analysis, stability analysis, and failure analysis of structures made from various materials such as metals, composites, and thin-walled structures [9-11]. In [12], this approach was used for common cases considering typical loadings with a random nature, as white noise and gusts. In this work, we use the same solution scheme based on finite element method with power spectral density. After the evaluation of the response of a sandwich cantilever beam and a laminated beam excited by a white noise in terms of PSD, the root mean square (RMS) values of the stresses were used to evaluate the failure index of the structures. The results were compared with those obtained using the commercial NASTRAN code.

2. One-dimensional finite elements

The one-dimensional (1D) model adopted in this work is based on the Carrera Unified Formulation (CUF). CUF allows writing the equations of any refined theory 1D, 2D, or 3D in terms of a few fundamental nuclei FN_s, whose shape does not depend on the assumptions used, such as type and order of the function, to describe the field of displacements. In the domain of CUF, the 3D displacement field of a solid beam with main dimension along the y-axis, can be expressed as a generic expansion of the generalized displacements $\mathbf{u}_\tau(\mathbf{y}, t)$:

$$\mathbf{u}(x, y, z, t) = F_\tau(x, z) \mathbf{u}_\tau(y, t), \quad \tau = 1, 2, \dots, M \quad (1)$$

where $F_\tau(x, z)$ are arbitrary functions on the cross-section, M stands for the number of the terms used in the expansion and repeated τ indicates summation. The generalized displacement can be approximated along the beam axis by discretizing the 1D support with finite elements to have:

$$\mathbf{u}_\tau(y, t) = N_i(y) \mathbf{u}_{\tau i}, \quad i = 1, 2, \dots, N_n \quad (2)$$

where the generalized displacements are described as a linear combination of the unknown nodal vector $\mathbf{u}_{\tau i}$ by 1D shape functions N_i and N_n is the number of structural nodes for each beam element. The expansion functions $F_\tau(x, z)$ are input parameters of the analysis and their

choice determines the class of the 1D CUF model. In this work, the Taylor (TE) and Lagrange (LE) expansion classes are adopted as polynomial bases. In the case of TE models, for example, F_τ functions are polynomials of the type $x^i z^i$ and the number of expansion terms is $M = (N + 1)(N + 2)/2$ with N is the order of TE model. For example, the full 3D displacement field of second-order model (TE2) is:

$$\begin{aligned} u_x &= u_{x_1} + xu_{x_2} + zu_{x_3} + x^2u_{x_4} + xzu_{x_5} + z^2u_{x_6} \\ u_y &= u_{y_1} + xu_{y_2} + zu_{y_3} + x^2u_{y_4} + xzu_{y_5} + z^2u_{y_6} \\ u_z &= u_{z_1} + xu_{z_2} + zu_{z_3} + x^2u_{z_4} + xzu_{z_5} + z^2u_{z_6} \end{aligned} \quad (3)$$

The classical beam theories can be derived as particular cases of the first order Taylor-like expansion (TE1). The first-order shear deformation theory (FSDT) is obtained neglecting the linear terms u_{x_2} , u_{x_3} , u_{z_2} , u_{z_3} and assuming the elastic rotations θ_z and ϕ_x equal to u_{y_2} and u_{y_3} . TE models sometimes can be inaccurate and thus are not suggested in the case of heterogeneous material or thin-walled structure. In this cases, Lagrange Expansion LE can be adopted, and the polynomial degree is determined by the number of nodes used to delimit each subdomain. Three-node linear (LE3), four-node bilinear (LE4), nine-node quadratic (LE9), and sixteen-node cubic (LE16) beam models have been developed in the CUF approach [6]. LE4 and LE9 cross-section elements are defined on quadrilateral domains. In the case of a LE9 element the interpolation functions are given by:

$$\begin{aligned} F_\tau &= 1/4(r^2 + rr_\tau)(s^2 + ss_\tau) \quad \tau = 1,3,5,7 \\ F_\tau &= 1/2s_\tau^2(s^2 - ss_\tau)(1 - r^2) + 1/2r_\tau^2(r^2 - rr_\tau)(1 - s^2) \quad \tau = 2,4,6,8 \\ F_\tau &= (1 - r^2)(1 - s^2) \quad \tau = 9 \end{aligned} \quad (4)$$

were r and s from -1 to +1.

Introducing the Principle of Virtual Displacement (PVD), it is possible to derive FE matrices and vectors by assembling the so-called *Fundamental Nuclei*, namely 3×3 matrices or 3×1 vectors. According to PVD, the virtual variation of the strain energy δL_{int} equals to the virtual variation of the work done by external loads δL_{ext}

$$\delta L_{int} = \delta L_{ext} \quad (5)$$

The virtual variation of the internal work can be written as:

$$\delta L_{int} = \delta \mathbf{u}_{sj}^T \int_V [N_{j(y)} F_s(x, z) \mathbf{D}^T \bar{\mathbf{C}} \mathbf{D} F_\tau N_i(y)] dV \mathbf{u}_{\tau i} = \delta \mathbf{u}_{sj}^T \mathbf{K}^{ij\tau s} \mathbf{u}_{\tau i} \quad (6)$$

where V is the body volume while \mathbf{D} and $\bar{\mathbf{C}}$ are, respectively, a differential operator and the matrix of the elastic coefficients of the linear geometrical and constitutive relations. The matrix

\mathbf{K}^{ijts} is the fundamental nucleus of the stiffness matrix. On the other hand, the work done by external forces can be written as

$$\delta L_{ext} = \int_V \delta \mathbf{u}^T \mathbf{F}_V dV + \int_A \delta \mathbf{u}_A^T \mathbf{F}_A dA + \delta \mathbf{u}_P^T \mathbf{F}_P \quad (7)$$

From the expression of the generalized forced in Eq. (7) is derived the cross-spectral density matrix \mathbf{S}_F .

2. Theory of random response

Considering a linear structural system with n degrees of freedom, the equation of motion can be written as:

$$\mathbf{M}\ddot{\mathbf{q}} + \mathbf{C}\dot{\mathbf{q}} + \mathbf{K}\mathbf{q} = \mathbf{f}(t) \quad (8)$$

Where \mathbf{M} , \mathbf{C} , \mathbf{K} are the mass, damping and stiffness matrices, $\mathbf{f}(t)$ is the time-dependent random force vector acting upon certain degrees of freedom, and $\ddot{\mathbf{q}}$, $\dot{\mathbf{q}}$, \mathbf{q} are the vectors of generalized acceleration, velocity, and displacement, respectively. Using the Fourier transformation of Eq. (8), it is possible to obtain the equation in frequency domain:

$$\mathbf{q}_k(\omega) = [-\omega^2 \mathbf{M} + i\omega \mathbf{C} + \mathbf{K}]^{-1} \mathbf{F}_k^* \quad i = \sqrt{-1} \quad (9)$$

Where \mathbf{q}_k is the column vector that collects degree of freedom (DOF) of the FE model, k is an arbitrary non-null generalized coordinate, \mathbf{F}_k^* is the generalized force vector in frequency domain and it has only one non-null term (equal to 1).

2.1 Normal mode approach

To reduce the computational cost, it is common practice to employ a modal reduction strategy. This method uses the mode shapes of the structure to uncouple the equations of motion (when no damping or only modal damping is used) and, depending on the number of modes computed and retained, reduce the problem size. This approach utilizes an arbitrary number (nm) of eigenvectors (\mathbf{x}_j) obtained from the undamped, homogeneous equation of motion:

$$[-\omega^2 \mathbf{M} + \mathbf{K}] \mathbf{x}_j e^{i\omega_j t} = \mathbf{0} \quad j = 1, \dots, nm \quad (10)$$

The eigenvectors can be collected in a $DOF \times nm$ matrix \mathbf{X} , so the Eq. (9) becomes

$$\mathbf{X}^T \mathbf{q}_k(\omega) = [-\omega^2 (\mathbf{X}^T \mathbf{M} \mathbf{X}) + i\omega (\mathbf{X}^T \mathbf{C} \mathbf{X}) + (\mathbf{X}^T \mathbf{K} \mathbf{X})]^{-1} \mathbf{X}^T \mathbf{F}_k^* \quad (11)$$

And it possible to obtain uncoupled equations, where $(\mathbf{X}^T \mathbf{M} \mathbf{X})$, $(\mathbf{X}^T \mathbf{C} \mathbf{X})$, $(\mathbf{X}^T \mathbf{K} \mathbf{X})$ are the modal generalized matrices.

2.1 Power spectral density

The Power Spectral Density (PSD) function of a signal gives an indication of the average power contained in particular frequencies [13]. It can be expressed in units of radians or in units of hertz and it is defined as

$$\mathbf{S}_{xx}(f) = \lim_{T \rightarrow \infty} \frac{1}{T} |\mathbf{x}_T(t)|^2 \quad (12)$$

where $\mathbf{x}_T(t)$ is the signal distribution over time. In the statistical approach, another quantity is employed. The Root Mean Square (RMS) which represents the mean value of the input signal, and it is the square root of the area below PSD curve:

$$RMS_{xx} = \sqrt{\int_{f_1}^{f_2} S_{xx}(f) df} \quad (13)$$

In frequency domain, given an input PSD function, an output response can be calculated by using the systems transfer function:

$$\mathbf{S}_{out} = |\mathbf{H}(\omega)|^2 \mathbf{S}_{in} \quad (14)$$

where $\mathbf{H}(\omega)$ is the system transfer function. In this case, the PSD of the three-dimensional displacement \mathbf{S}_u and the stress \mathbf{S}_σ components at various frequencies (ω) are correlated with the PSD of the load \mathbf{S}_F by the following equations

$$\begin{aligned} \mathbf{S}_{u_i}(\omega) &= \bar{\mathbf{H}}_{u_i}(\omega) \mathbf{S}_F(\omega) \mathbf{H}_{u_i}^T(\omega) & i = 1,2,3 \\ \mathbf{S}_{\sigma_j}(\omega) &= \bar{\mathbf{H}}_{\sigma_j}(\omega) \mathbf{S}_F(\omega) \mathbf{H}_{\sigma_j}^T(\omega) & j = 1, \dots, 6 \end{aligned} \quad (15)$$

where $\bar{\mathbf{H}}(\omega)$ and $\mathbf{H}^T(\omega)$ are the complex conjugate and the transpose of the transfer function also called admittance matrix. It can be computed with the FE method by performing as many frequencies response analysis as of the non-null terms (nnz) in the generalized force vector F . For an arbitrary non-null generalized coordinate (k), the matrix is

$$\mathbf{H}_{q_k}(\omega) = [\mathbf{q}_{k1} \ \mathbf{q}_{k2} \ \dots \ \mathbf{q}_{kL}] \quad k = 1, \dots, nnz \quad L = 1, \dots, fs \quad (16)$$

where \mathbf{q} is derived from the Eq. (9) and fs is the number of frequency steps. In this work, structures subjected to white noise excitations are considered, thus the PSD of this type of noise is constant.

3. Numerical results

3.1 Sandwich beam

The first numerical example refers to the response of a sandwich cantilever beam subjected to a clipped white noise built as four-point loads (1 N) as shown in Fig. 1. Table 1 lists the geometrical and material data of the soft-core (indicated with the subscript “c”) and the metallic faces (indicated with the subscript “f”).

Geometrical data	Material data
L=0.1 m	$E_f = 200.0 \text{ GPa}$ $E_c = 0.66 \text{ GPa}$
h = b = 0.02 m	$\nu_f = 0.27$ $\nu_c = 0.3$
$h_c = 0.014 \text{ m}$	$\rho_f = 7800 \text{ kgm}^{-3}$ $\rho_c = 60 \text{ kgm}^{-3}$

Table 1. Geometrical and material data of sandwich beam.

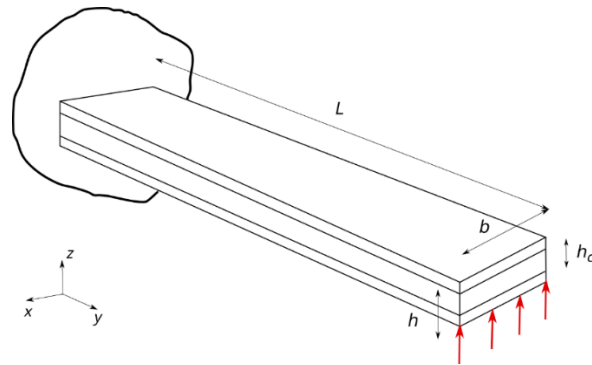


Figure 1. Boundary condition and geometry of the sandwich beam subjected to clipped white noise.

Fourteen four-nodes beam elements were used along the longitudinal axis and the displacement variables on the cross-section were approximated with the TE2, TE3, TE6, and 3-LE16 models. To verify the accuracy of the model the results are compared with solutions obtained by commercial code NASTRAN. At first, a normal mode analysis was implemented. In Table 2, the first ten natural frequencies are listed and compared with frequencies obtained by a model of 12915 Degrees of Freedom (DoFs) on NASTRAN. In Fig. 2, some of normal modes are shown.

Frequency	3-LE16 CUF [Hz]	NASTRAN [Hz]
1	905.58	905.65
2	1586.28	1586.54
3	2248.23	2232.41
4	3040.16	3039.71
5	6082.35	6078.87
6	8476.70	8376.37
7	8583.21	8580.41
8	10140.59	10005.23
9	10174.15	10134.30
10	10733.98	10490.53

Table 2. First ten natural frequencies of sandwich beam. Comparison between 3-LE16 CUF and NASTRAN solutions.

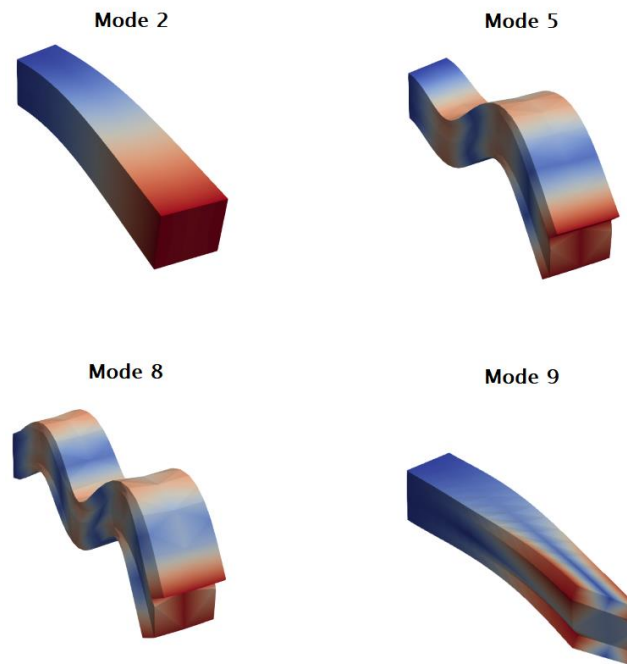


Figure 2. Some normal modes of sandwich beam.

A normal modes analysis is the starting point for all linear dynamic work and can help to capture how much mass is associated with each natural frequency. Therefore, before the PSD analysis, it should be useful to evaluate the mass participation to accurately capture the dynamic response of the structure.

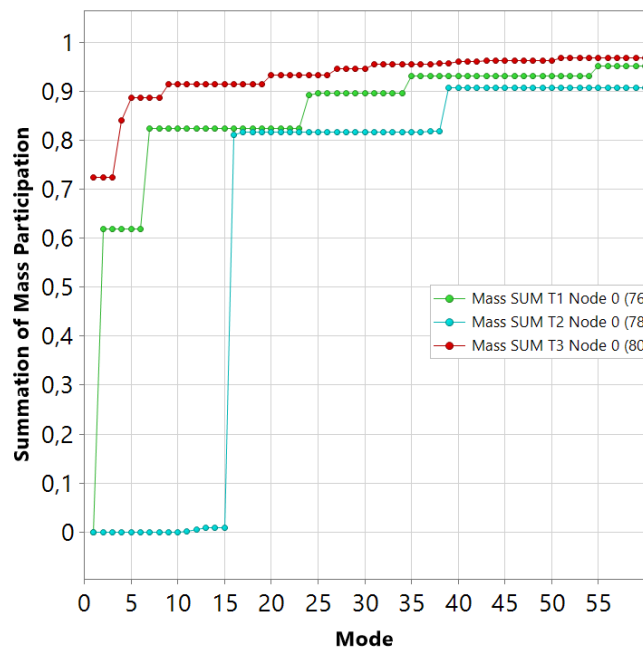


Figure 3. Mass participation versus number of modes of the sandwich beam response.

To ensure that we have captured the dynamic response of the structure, it should be useful to use enough modes that at least 90 % of the mass of the structure is covered. In Fig. 3, it is possible to notice that 40 modes are necessary to capture at least 90 % of dynamic response of

the structure. Therefore, starting from the modal analysis, it is possible to compute a PSD analysis. This approach is statistical, and it is just a sophisticated and extremely useful form of the modal frequency analysis. Rather than having to examine multiple sets of results, the PSD approach employs a broad-spectrum acceleration load to activate the structure and subsequently consolidates the solutions into a single, unified result. To capture a correct dynamic response, 45 modes are used in modal frequency analysis.

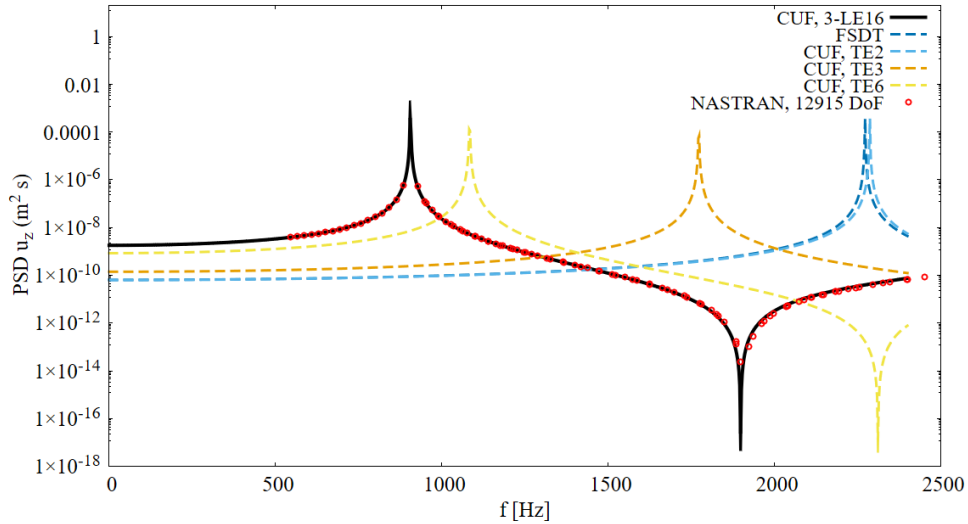


Figure 4. Power spectral density of the vertical displacement at the tip of the beam ($\frac{b}{3}, L, \frac{h}{2}$). Comparison with various theories and solution obtained by NASTRAN with a solid beam model of 12915 Degrees of Freedom (DoFs).

In Fig. 4, the power spectral density of the vertical displacement at the tip of the beam with $x=b/3$ is shown. It can be observed that the frequency corresponding to the peak related to the first natural mode is overestimated in the case of Taylor theories, especially for smaller orders.

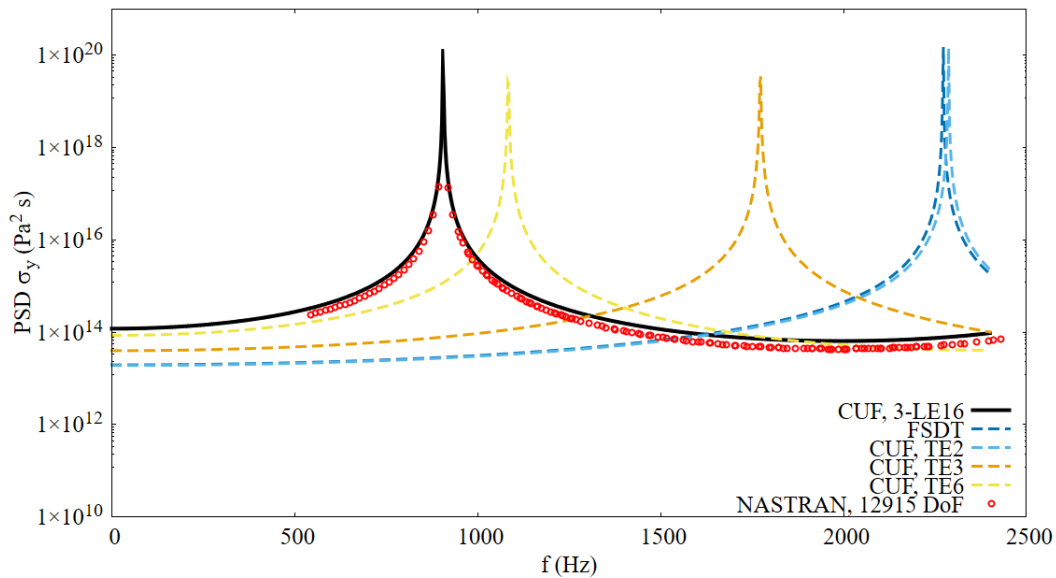


Figure 5. Power spectral density of axial normal stress σ_{yy} of point close to the clamped edge ($0, 0.0025, \frac{h}{2}$).

In Fig. 5, the power spectral density of the axial normal stress σ_{yy} of the point close to the clamped with coordinates $(0, 0.0025, h/2)$. As for PSD of displacement, the Taylor theories overestimates frequencies of the first natural mode. This happen because the structure appears stiffer than the reality. By increasing the order of expansion, the solution becomes progressively more accurate. As shown, the CUF approach with 3-LE16 correctly described the behavior of the structure and it coincides with the PSD response obtain by NASTRAN. Note that the displacement and stress results are referred to 1- σ responses. The σ refers to a Gaussian distribution where 1- σ to 3- σ refers to, 68, 95 and 99.7 % ranges. At 3- σ for examples, there is the 99.7 % that the stresses are within this value, where σ represents the Root Mean Square (RMS) of the stress. In this case, an undamped model is considered.

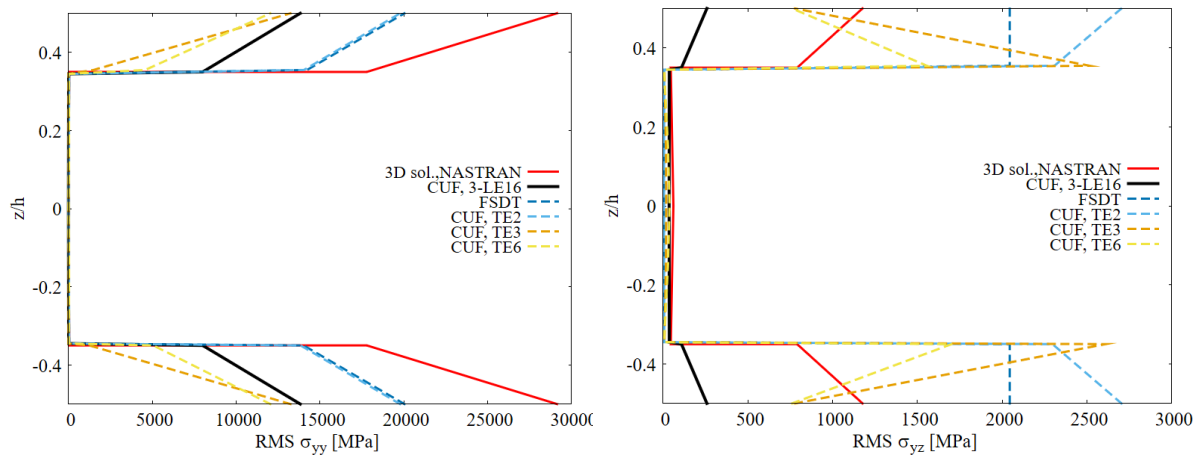


Figure 6. Root mean square of the axial stress and transverse shear stress through the thickness at $(0, 0.0025, z)$.

In Fig. 6, it is possible to notice that NASTRAN solution is bigger than CUF-FEM solution because of the integration. As mentioned before, the root mean square is the root of the area under the PSD curve and RMS computed by NASTRAN has bigger values of PSD corresponding to the peak. Thus, the difference between the solutions is caused by these different values of peaks. From the RMS values of stress, considering 3-RMS of each layer and substituting them in one of the composite failure criteria, it is possible to evaluate the safety of beam under white noise excitation and the failure index. In Fig. 7, the root mean square map of the axial stress is shown.

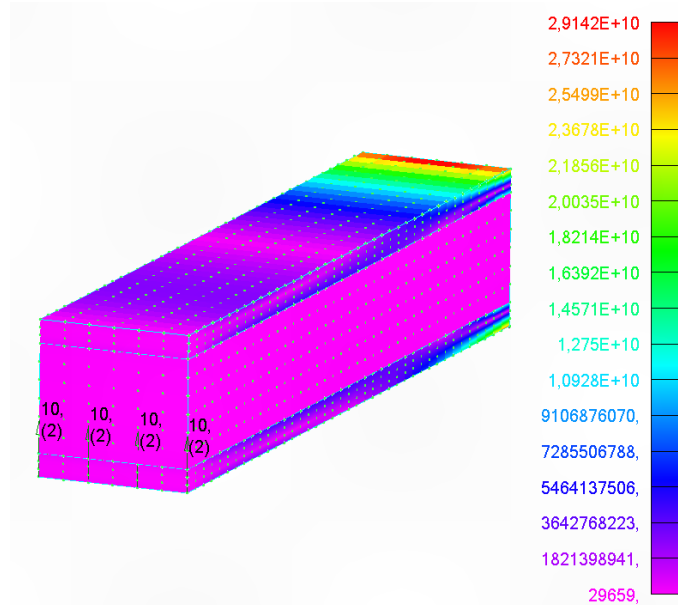


Figure 7. Root mean square map of axial stress σ_{yy} [Pa] on NASTRAN of the sandwich beam under clipped white noise.

3.1 Laminated beam

The second numerical example refers to a clamped-free laminated beam subjected to axial loads, Fig. 8.

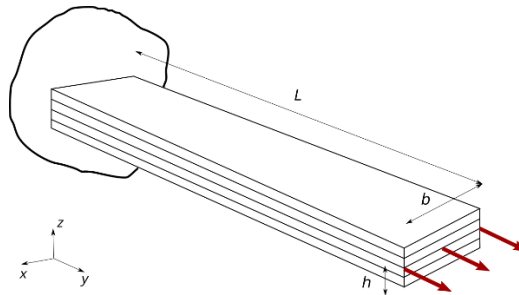


Figure 8. Boundary condition and geometry of the laminated beam subjected to axial loads.

In Table 3, the material and geometric data are listed. The beam has the following dimensions $L = 400$ mm, $b = 0.02$ mm, and $h = 0.005$ m. We considered a symmetric cross-ply with four layers of equal thickness, $h_i = h/4$ and lamination $[0, 90]_s$. The present assessment consists of 6 cubic 1D elements along the beam axis and a distribution of quadratic LE over the cross-section domain which in all cases consists of quadratic 10 LE9 in the x-axis with a graded distribution towards both the free edges. A convergency study is performed, considering from one LE per layer up to four LE per layer.

Geometrical data	Material data
$L=0.400$ m	$E_1 = 137.9$ GPa $E_2=E_3 = 14.5$ GPa
$b = 0.02$ m	$\nu_{12} = \nu_{13} = \nu_{23} = 0.21$
$h = 0.005$ m	$\rho_f = 1570$ kgm ⁻³
	$G_{12} = G_{13} = G_{23} = 5.9$ GPa

Table 3. Geometrical and material data of laminated beam.

In Fig.9 and Fig.10, the power spectral density of the axial displacement and axial stress at the point $(b/2, L/2, h/2)$ are shown. The convergence is achieved already for 1-LE per layer. Instead, in Fig. 11, the root mean square of the axial stress σ_{yy} and the shear stress σ_{xy} are plotted. As shown, the convergence is achieved for 2-LE per layer. As for the previous example, at 3-RMS there is the 99.7 % that the stresses are within this value and this value could be used in the failure criteria.

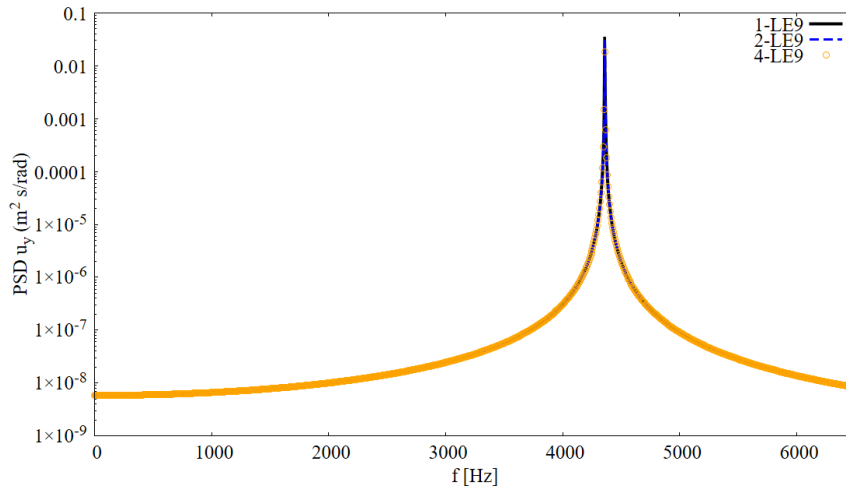


Figure 9. Power spectral density of the axial displacement of the laminated beam at point $(b/2, L/2, h/2)$.

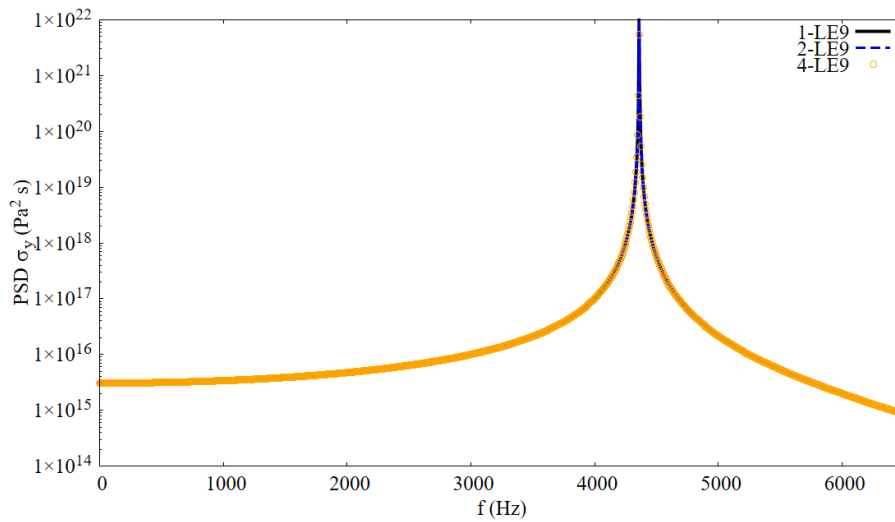


Figure 10. Power spectral density of axial normal stress σ_{yy} of the laminated beam at the point $(b/2, L/2, h/2)$.

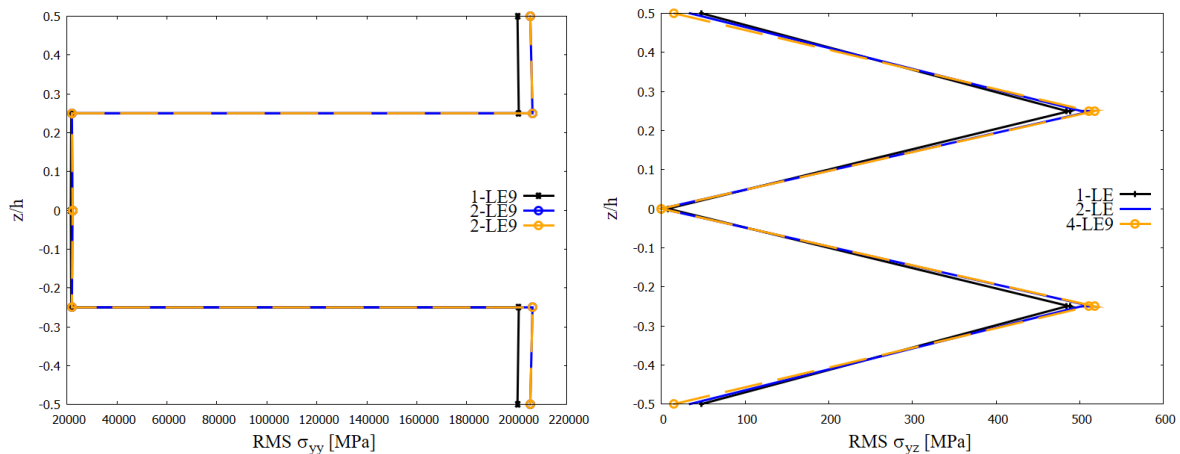


Figure 11. Root mean square distribution along thickness of the axial stress σ_{yy} and transverse shear stress σ_{xy} at $y=L/2$.

4. Conclusion

This paper investigated the use of advanced finite beam elements to accurately described the dynamic responses of composite structures under random excitations. Using the one-dimensional models with CUF approach and exploiting higher order theories. Starting from a normal mode analysis, results are given in terms power spectral densities and root mean square of displacement and stress. The RMS stress values could be employed in the fatigue criteria of composite. The numerical investigation included a sandwich beam under transverse clipped white noise and a laminated beam under axial white noise. The results show that this 1D approach is an advantageous and computationally lighter alternative than 3D approach used, for example, by commercial code as NASTRAN.

References

- [1] Reytier T., Bes C., Marechal P., Bianciardi M., Santgerma A. Generation of correlated stress time histories from continuous turbulence Power Spectral Density for fatigue analysis of aircraft structures. *International Journal of Fatigue*, 42, pp 147-152 (2012).
- [2] Muñiz-Calvente M. A comparative review of time- and frequency-domain methods for fatigue damage assessment. *International Journal of Fatigue*, 163, 107069 (2022).
- [3] Halfpenny, A. A frequency domain approach for fatigue life estimation from finite element analysis. *Key Engineering Materials*, 167, pp 401-410 (1999).
- [4] Rafiee R., Sharifi P. Stochastic failure analysis of composite pipes subjected to random excitation. *Construction and Building Materials*, 224, pp 950-961 (2019).
- [5] Newsom C., Fullera J., Sherrer R. *A finite element approach for the analysis of randomly excited complex elastic structures* in “8th Structural Dynamics and Materials Conference”, (2012).
- [6] Olson M. D., A consistent finite element method for random response problems. *Computers & Structures*, 2, pp 163-180 (1972).

- [7] Dey, S. S., Finite element method for random response of structures due to stochastic excitation, *Computer Methods in Applied Mechanics and Engineering*, Vol. 20, No. 2, pp. 173–194 (1979).
- [8] Goswami, S., Response of composite stiffened shells under stochastic excitation, *Journal of reinforced plastics and composites*, Vol. 16, No. 16, pp. 1492–1522 (1997).
- [9] Petrolo M., Carrera E., Cinefra M., Zappino E. Finite element analysis of structures through unified formulation. *John Wiley & Sons* (2014).
- [10] Carrera E., Zappino E., Carrera E. Unified Formulation for Free-Vibration Analysis of Aircraft Structures. *AIAA Journal*, pp 1–13, (2015).
- [11] Wu B., Pagani A., Filippi M., Chen W., Carrera, E. Large-deflection and post-buckling analyses of isotropic rectangular plates by Carrera Unified Formulation, *International Journal of Non-Linear Mechanics*, Vol. 116, pp. 18–31 (2019).
- [12] Filippi M., Petrolo M., Carrera E. *Refined structural theories for the random response of fiber-reinforced and sandwich composite structures* in “AIAA SCITECH 2022 Forum”, (2022).
- [13] Bishop N. W. M., Sherratt F. Fatigue life prediction from power spectral density data. *Environmental Engineering*, pp. 2-11 (1989)